

Geochemical implication for the maximum flooding of the Jomon transgression in the coastal lagoon sediments, San'in district, SW Japan

Hiroaki Ishiga*, Tadashi Nakamura*, Yoshikazu Sampei*, Takao Tokuoka* and Katsumi Takayasu**

Abstract

The Holocene Jomon transgression was recorded in sediments at the archeological site in the Shimane University, which were deposited in the most inner part of the lagoon. Marine mud deposition in back marsh condition indicates start of the transgression, which is marked by the Kikai-Akahoya tephra of 6300 yrs BP.

Marine muds are characterized by fluctuating values of LOI (loss on ignition), total sulfur contents (TS), and $\text{Fe}_2\text{O}_3/\text{Al}_2\text{O}_3$ ratios and these values are relatively higher than those of the non-marine ones in this section. Rb/K also shows fluctuation, indicating Rb enrichment in under marine condition, probably related to Rb adsorption on clays. The sediments of this section show higher CIA (80~85) suggesting derivation of highly weathered material from the source or sorting of the clays. Ti/Zr shows gradual increase in the Jomon age, suggesting heavy mineral fractionation related to the transgression.

High stand in sea-level probably lasted until middle Jomon age (4500 yrs BP), and consequently effects of fluvial inputs were dominated due to lowered sea-level. Gradual decrease in $\text{Al}_2\text{O}_3/\text{TiO}_2$, $\text{SiO}_2/\text{Al}_2\text{O}_3$ and Ti/Zr, and increase in Nb/Y and Zr/Y may be related to the source compositional changes due to the widening of the paddy field in the Yayoi age from 2400 yrs BP.

Key words: Holocene, coastal lagoon, Jomon transgression, organic muds, geochemistry

Introduction

The Jomon transgression was evaluated by examination of the distribution of shell mound in the Kanto Plain, and the level of maximum flooding was two meters higher than that of the present level (Ota and Yonekura, 1987). The environmental change clearly appears in lithology, namely, coarser sediments gradually change into organic black muds. These muds are characterized by higher concentration of total sulfur (TS=over 0.3%) which was trapped in sediments under sulfur reducing reaction in anoxic condition (Berner, 1984). Thus TS concentration, and total organic carbon / TS ratios (TOC/TS=over 5) are useful indicator of marine condition (Berner and Raiswell, 1984 ; Sampei et al., 1997). To evaluate sedimentary environment, TS and TOC are utilized in the coastal lagoon sediments, because they had an effect of frequent sea-level changes during the Holocene (Sampei et al., 1997).

The invasion of sea-water into the coastal plain resulted in environmental change which may have re-

flected in geochemical change of sediments. However, geochemical composition may be influenced by grain size fractionation (Taylor and McLennan, 1985; McLennan et al., 1993; Garcia et al., 1994), thus muds deposited in back swamp condition were utilized for this analysis. This is because swamp is usually barriered from direct effect of fluvial detritus due to dense vegetation.

Geologic outline of the Nakaumi and Shinjiko lagoons

The Lakes Nakaumi and Shinji have remained as brackish lakes after the last sea-level rise in Jomon age (Tokuoka et al., 1990), which initiated at 10 k yrs BP (Ota and Yonekura, 1987; Ota et al., 1982; Umitsu, 1991) (Fig.1). This transgression was followed by the Yayoi fall in sea-level (2400 yrs BP) (Tokuoka et al., 1990). Sea water invasion was recorded in many archeological sites in the coastal lagoons, where black muds with higher concentration of total sulfur and total organic carbon were formed (Nakamura and Tokuoka, 1997; Sampei et al., 1996). Sediments deposited during the Jomon transgression is called Shinjiko Formation in the coastal region of Lake Shinji (Tokuoka et al., 1995), and gradually changed into coarser clastics (Tokuoka et al., 1990).

* Department of Geoscience, Shimane University, Matsue 690-8504, Japan

** Research Center for Coastal Lagoon, Shimane University, Matsue 690-8504, Japan

The previous lagoonal environment was probably influenced by fresh water to produce brackish condition, and coastal plains were expanded in this region (Fig. 1).

The examined section of the archeological site in the

Shimane University is situated in the most inner part of the Shinjiko lagoon, and the Tertiary basement rocks are distributed. The Shinjiko Formation overlaps the Tertiary rocks.

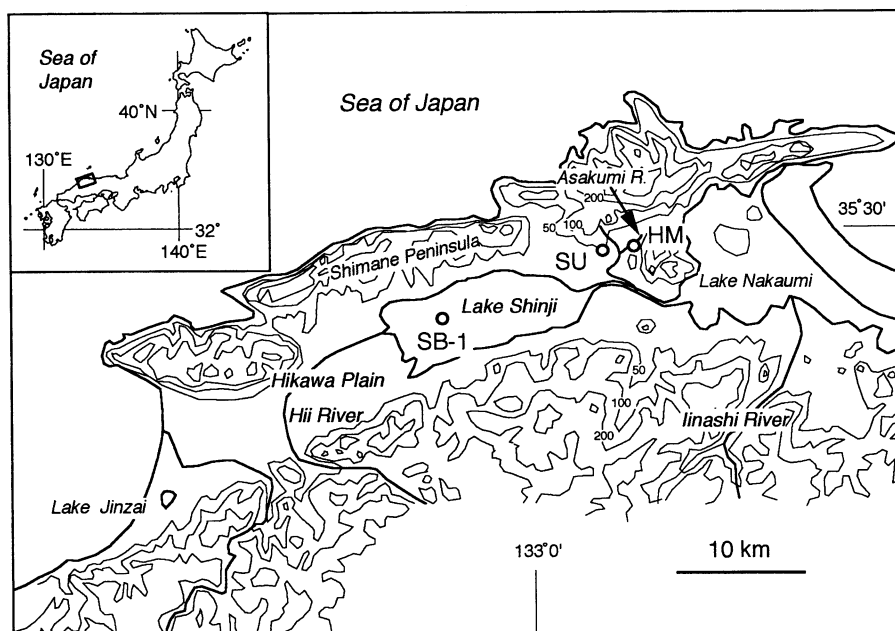


Fig. 1 Location of SU (Shimane University) section and topography of Shinji-Nakaumi lagoon, San'in district of Southwest Japan. Locations of HM section (Haranomae archeological site) of the Asakumi River and SB-1 of Shinjiko boring samples are also shown.

Mud samples of the Shimane University

Mud samples were collected at an archeological site in Shimane University (SU section). The 3.5 m section is characterized by the occurrence of alternating beds of black and white-gray muds (Figs. 2, 3). The muds unconformably overlies basic Tertiary pyroclastics. The surface of the unconformity dips 20 degrees to the south, and undulates.

Stratigraphy

According to lithology and archeological material, the column is subdivided into 7 beds in ascending order (Figs 4 and 5). Bed 7 muds show gray in color, while bed 6 consists of alternation of black muds and white muds with individual beds several cm thick. Beds 5 and 4 are white and black muds, respectively, and bed 3 muds are yellow and also has sands. Mud at this site are rich in higher plant remains, especially so far black muds. Diatoms occur in both black and white beds. Considering dominance of plant remains,

absence of coarser clastics, and low sedimentation rates, muds in this section are inferred to have been deposited in back marsh conditions with influence of marine invasion shown by total sulfur contents as discussed later.

Age

The K-Ah tephra (6300 yrs BP) is intercalated between beds 7 and 6. Bed 3 yielded middle Yayoi remains (2100 yrs BP), and intercalation of coarse clastics may be related to lowered sea-level in Yayoi age.

Slow sedimentation rate (SR=0.08 cm/yr) after 6300 yrs BP can be inferred, which is significantly lower than that of Lake Nakaumi (0.11~0.37 cm/y) after 6300 yrs BP as determined by Sampei et al. (1996).

Sample preparation and analytical method

Mud samples from the SU section were collected at 10 cm intervals (n=37) for analysis. Dried samples (at 110°C for 24 hours) were utilized for analysis of total

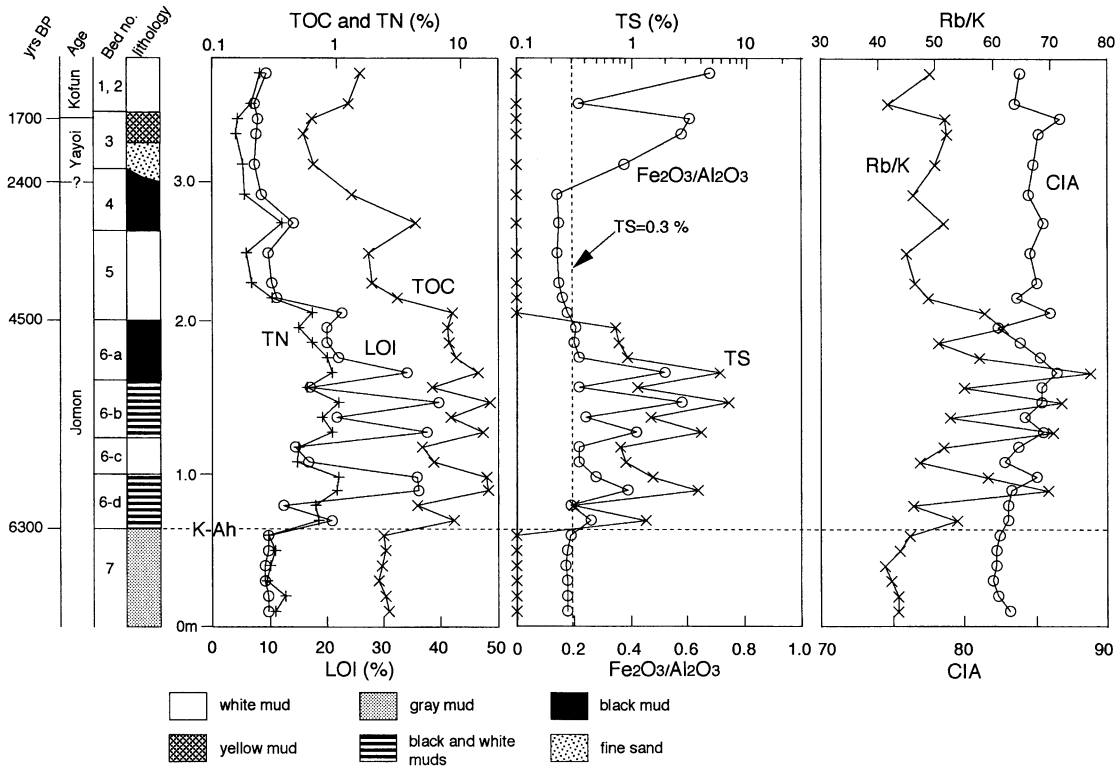


Fig. 2 Stratigraphic variation of LOI, TOC, TN, TS, $\text{Fe}_2\text{O}_3/\text{Al}_2\text{O}_3$, CIA and Rb/K of the muds at the archaeological site in Shimane University (SU section), San'in district of Southwest Japan. K-Ah represents Kikai-Akahoya tephra of 6300 yrs BP. Bed numbers are indicated.

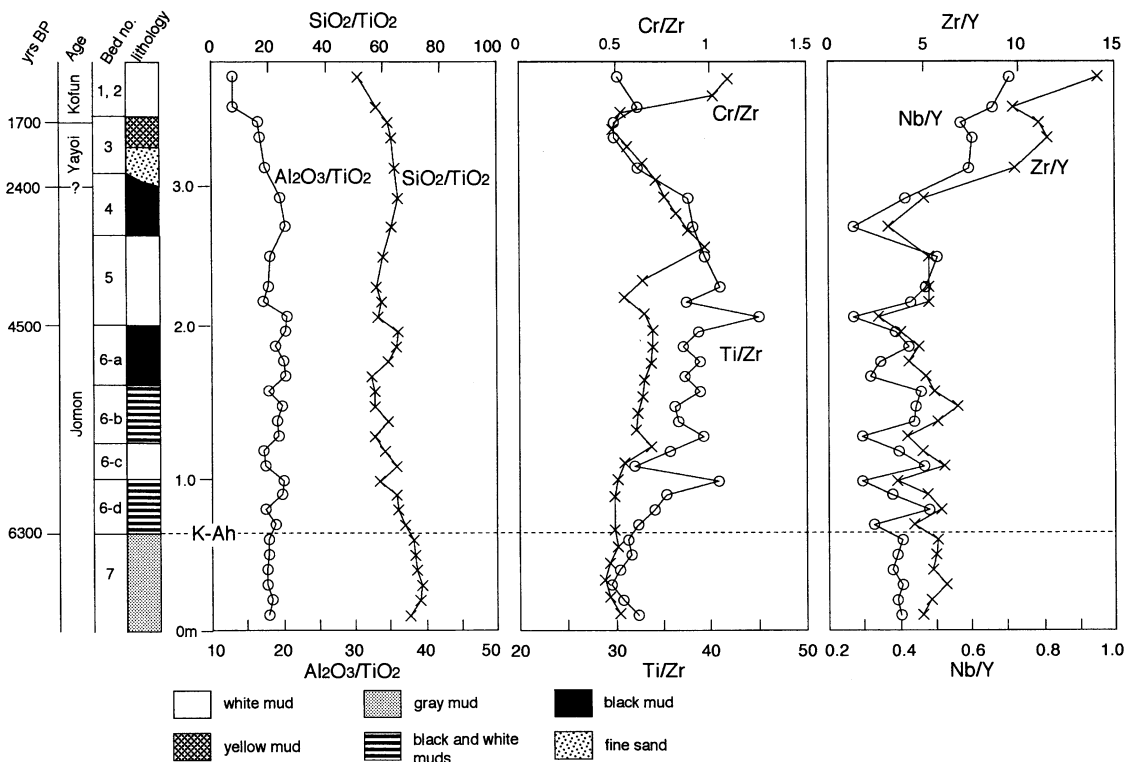


Fig. 3 Stratigraphic variation of $\text{Al}_2\text{O}_3/\text{TiO}_2$, $\text{SiO}_2/\text{Al}_2\text{O}_3$, Ti/Zr, Cr/Zr, Nb/Y and Zr/Y of the muds at the archaeological site in Shimane University (SU section), San'in district of Southwest Japan. K-Ah represents Kikai-Akahoya tephra of 6300 yrs BP.

organic C, total N and total S, and major and trace elements.

Total organic carbon and total nitrogen

Total organic carbon (TOC), and total nitrogen (TN) were measured using a CHN-corder (Yanako MT-3). The method is outlined in Suzuki et al. (1986) and Sampei (1991).

Total Sulfur

Total sulfur (TS) was measured on 200 mg samples by combustion and infrared absorption spectrometry using a HORIBA EMIA-120, following the procedure of Terashima (1979). The errors (coefficient of variation) inherent to this analysis were less than 3%.

Major and trace elements

Major elements (SiO₂, TiO₂, Al₂O₃, Fe₂O₃*, MnO, MgO, CaO, Na₂O, K₂O, and P₂O₅) and trace elements (V, Cr, Co, Ni, Cu, Zn, Y, Zr, Nb, Rb, Sr, and Ba) were analyzed using the RIX 2000 XRF system (Rigaku Denki Co. Ltd.) of Shimane University. Analysis were made on glass beads prepared with lithium tetraborate flux with a flux to sample ratio of 5:1, fundamentally followed by Norrish and Hutton (1969).

Results are given in Table 1. For analytical errors, standard deviations of analyzed values (n=10) of USGS standard SCo-1 (Cody Shale) are shown in comparison with preferred values from Potts et al. (1992).

L O I (Loss on ignition)

Loss on ignition was determined by ignition of powdered samples at 1100°C in a muffle furnace for 1 hour.

Geochemical characteristics of the Holocene muds

LOI, TOC, TN and TS

Muds of bed 7 show consistent values in LOI, TOC, TN and TS, and change their values at the boundary of beds 7 and 6. Within the bed 6, they show fluctuation and black muds have higher concentration in LOI (over 35%), TOC (over 10%), TN (over 1%) and TS (over 1%) relative to those of white muds. Variation of these elements in bed 6 correlate well with Fe₂O₃/Al₂O₃ and Rb/K ratios. Higher TOC and TOC/TN (~16.2) are suggestive of enriched organic matter probable derived from higher plants. High TOC/TS (~10.9) and increase in Fe₂O₃/Al₂O₃ are suggestive of deposition under marine condition in previous swamp

Table 1 Analyses of the muds at the archeological site in SU section (Shimane University), San'in district of Southwest Japan. Numbers are sample numbers in stratigraphically descending order with 10 cm thick intervals. -: less than 0.01% for TS. Total Fe is given as Fe₂O₃.

Bed no.	sample no.	Oxides (wt. %)											Trace elements (ppm)											wt. %			
		SiO ₂	TiO ₂	Al ₂ O ₃	Fe ₂ O ₃	MnO	MgO	CaO	Na ₂ O	K ₂ O	P ₂ O ₅	Total	LOI	V	Cr	Ni	Cu	Zn	Y	Zr	Nb	Rb	Sr	Ba	TOC	TN	TS
Bed 1, 2	SU-1	66.09	1.29	16.81	11.37	0.10	1.09	0.55	0.56	1.32	0.05	99.24	9.38	139	282	71	18	59	18	257	13	78	66	309	1.54	0.24	-
	SU-3	73.91	1.28	16.86	3.66	0.03	1.05	0.40	0.67	1.45	0.03	99.34	7.47	139	241	51	19	65	25	237	16	73	76	358	1.24	0.20	-
Bed 3	SU-4	66.18	1.07	17.81	10.91	0.02	1.06	0.30	0.45	1.49	0.08	99.37	7.80	122	114	39	09	83	20	215	11	93	53	340	0.63	0.16	-
	SU-5	66.66	1.06	17.66	10.18	0.07	1.14	0.36	0.54	1.54	0.07	99.29	7.70	138	102	37	08	84	19	212	11	96	57	371	0.53	0.16	-
Bed 4	SU-7	68.58	1.07	18.72	7.08	0.08	1.25	0.42	0.57	1.65	0.06	99.48	7.40	119	113	33	08	82	20	199	12	99	65	384	0.64	0.17	-
	SU-9	70.70	1.08	21.07	2.91	0.04	1.33	0.48	0.62	1.89	0.03	100.16	8.64	109	111	33	15	87	34	172	14	105	91	507	1.33	0.18	-
Bed 5	SU-11	68.90	1.10	22.42	3.27	0.04	1.52	0.53	0.50	1.88	0.01	100.15	14.23	156	123	41	32	110	54	172	15	117	82	552	4.33	0.36	-
	SU-13	69.81	1.17	21.25	3.07	0.03	1.50	0.44	0.59	2.04	0.05	99.95	9.85	138	135	32	18	128	34	177	17	111	77	518	1.81	0.19	-
Bed 5	SU-15	69.27	1.21	21.67	3.29	0.04	1.59	0.46	0.59	1.97	0.05	100.13	10.25	138	145	36	22	94	33	177	16	110	80	560	1.94	0.20	-
	SU-16	70.12	1.19	20.46	3.36	0.04	1.54	0.51	0.63	2.00	0.06	99.89	11.27	141	167	38	25	86	36	190	15	118	86	529	3.08	0.30	-
Bed 5	SU-17	66.05	1.14	23.49	4.17	0.06	1.77	0.67	0.39	1.97	0.08	99.79	22.77	207	147	51	62	127	57	151	16	139	84	525	8.51	0.63	-
	SU-18	68.02	1.04	21.30	4.50	0.06	1.57	0.95	0.62	1.83	0.08	99.97	20.08	141	104	62	34	38	43	161	17	136	145	533	7.77	0.49	0.72
Bed 6a	SU-19	69.49	1.08	20.47	4.13	0.05	1.42	0.68	0.49	1.92	0.07	99.79	19.92	123	95	43	24	-	37	174	16	117	95	548	8.13	0.63	0.78
	SU-20	67.60	1.10	22.12	4.89	0.06	1.54	0.81	0.37	1.78	0.09	100.36	22.05	135	111	46	27	12	40	169	14	124	96	538	9.05	0.84	0.91
Bed 6b	SU-21	60.31	1.08	22.05	11.49	0.06	1.65	0.81	0.30	1.60	0.10	99.44	34.12	223	120	161	54	179	34	173	11	148	85	502	13.74	0.91	5.89
	SU-22	67.98	1.19	21.42	4.62	0.04	1.61	0.58	0.44	1.88	0.07	99.83	17.10	120	127	53	28	100	33	183	15	125	84	514	5.93	0.57	1.10
Bed 6b	SU-23	60.28	1.06	21.06	12.13	0.05	1.73	0.77	0.37	1.70	0.10	99.24	39.78	215	120	168	46	91	26	175	11	147	79	467	16.89	1.05	6.88
	SU-24	67.73	1.09	20.93	5.08	0.04	1.72	0.61	0.47	2.04	0.07	99.79	21.75	158	117	47	29	-	31	179	14	130	83	498	8.42	0.75	1.46
Bed 6c	SU-25	63.32	1.11	21.42	8.96	0.06	1.74	0.86	0.36	1.59	0.11	99.53	37.60	195	109	97	53	05	41	169	12	135	86	510	15.12	0.91	4.02
	SU-26	69.95	1.16	19.86	4.30	0.04	1.49	0.56	0.55	1.92	0.06	99.88	14.32	131	120	61	20	107	39	194	15	119	83	493	4.95	0.49	0.79
Bed 6c	SU-27	70.82	1.10	19.12	4.19	0.04	1.49	0.51	0.56	2.07	0.06	99.95	16.65	131	126	38	26	131	34	206	16	118	80	471	6.20	0.48	0.88
	SU-28	65.27	1.11	22.30	6.14	0.05	1.81	0.85	0.38	1.86	0.11	99.87	35.90	198	112	60	46	69	45	163	13	132	86	519	16.30	1.04	1.49
Bed 6d	SU-29	65.54	1.00	20.03	7.88	0.05	1.65	0.84	0.42	1.86	0.09	99.36	36.22	161	93	61	33	60	33	172	13	157	85	477	16.35	1.01	3.77
	SU-30	71.42	1.09	19.11	3.68	0.03	1.46	0.46	0.58	2.05	0.05	99.94	12.46	117	98	40	16	47	33	192	16	114	74	466	4.53	0.66	0.32
Bed 6d	SU-31	69.56	1.03	19.41	5.00	0.04	1.40	0.64	0.60	1.85	0.07	99.59	20.99	149	94	56	29	171	43	191	14	120	78	502	8.95	0.71	1.34
	SU-32	72.14	1.02	18.38	3.50	0.03	1.37	0.46	0.62	2.02	0.05	99.58	9.59	119	97	33	16	95	34	195	14	111	73	466	2.38	0.28	-
Bed 7	SU-33	72.68	1.02	18.29	3.30	0.03	1.27	0.46	0.65	1.99	0.05	99.74	9.70	125	99	28	16	168	34	194	13	105	75	467	2.45	0.32	-
	SU-34	73.19	1.02	18.12	3.05	0.03	1.19	0.45	0.66	1.96	0.05	99.70	9.16	116	94	32	22	82	36	200	14	97	74	453	2.32	0.29	-
Bed 7	SU-35	73.39	1.00	17.74	3.15	0.03	1.21	0.45	0.68	1.93	0.05	99.61	9.09	103	91	26	18	103	33	204	13	98	74	445	2.19	0.27	-
	SU-36	72.54	1.00	18.36	3.34	0.03	1.30	0.45	0.63	2.02	0.05	99.72	9.61	107	91	32	25	112	36	194	14	106	73	468	2.50	0.38	-
Bed 7	SU-37	72.05	1.04	18.81	3.31	0.03	1.27	0.45	0.60	1.98	0.06	99.59	9.83	118	101	33	21	92	39	192	16	104	73	455	2.63	0.32	-

during deposition of bed 6. LOI, TOC, TN and TS values of bed 5 decrease to similar level of bed 7 with some variation. This change may indicate sea-level fall and returning to non-marine condition. Higher values in $\text{Fe}_2\text{O}_3/\text{Al}_2\text{O}_3$ of bed 3 without relation to TS is perhaps due to diagenetic enrichment in Fe_2O_3 .

SiO₂

SiO₂ concentration may be related to maturation of sediments, grain size and biogenic silica contamination (e.g. McLennan et al., 1993). Thus SiO₂ usually shows negative correlation with Al₂O₃ which represents clay contents. Muds of the examined section show weak negative correlation between SiO₂ and Al₂O₃ ($r^2=0.50$). High concentration of Al₂O₃ over 20 wt% may be related to enrichment of clays in the sediments.

Alkali and alkaline earth elements

Na₂O, CaO and K₂O show variation in the section which were affected by effects of weathering, sorting and absorption. Na₂O has negative correlation with Al₂O₃ ($r^2=0.61$), suggestive of presence of Na rich-feldspar or albitization of feldspar. Ca shows weak correlation with Al₂O₃ ($r^2=0.64$), but K₂O has no correlation to Al₂O₃. Mg ($r^2=0.84$), Rb ($r^2=0.67$) and Ba ($r^2=0.78$) show correlation to Al₂O₃ (Fig. 4), suggesting effect of adsorption on clays of these elements. Sr has no correlation to Al₂O₃. Rb and Ba are depleted in beds 2, 1 compared to those of the other samples, probably due to less concentration of clays in mud samples.

TiO₂, Zr, Nb and Y

These elements are generally immobile during weathering process, but they may vary in concentration due to grain-size fractionation. TiO₂ shows weak correlation with Al₂O₃ ($r^2=0.59$) excluding two samples of beds 2, 1 (Fig. 4), which have the highest (1.28 and 1.29%) values in the samples. Al₂O₃/TiO₂ and SiO₂/TiO₂ show small variation in bed 7 and vary slightly in beds 6 to 4 (Fig. 3). Clear decrease in these ratios occurs from bed 3 to 1. Although TOC, Fe/Al and TS show variation in the section, these immobile element ratios are relatively consistent.

Zr shows negative correlation with Al₂O₃ ($r^2=0.89$) (Fig. 4), and the uppermost two samples in bed 2 plot off this correlation line with least values of Al₂O₃. Zr, however, shows no correlation to TiO₂, suggesting that TiO₂ may be included as heavy minerals such as rutile

or titanite. Ti/Zr shows gradual increase from bed 7 to bed 6, and decreases toward the top of the section (Fig. 3).

Nb/Y and Zr/Y correlate well with each other in the section, and show some variations from bed 7 to 5. They subsequently increase from bed 4 to bed 2. Nb shows no clear correlation with Al₂O₃, but Y does show weak correlation ($r^2=0.67$). In this context, increase in Nb/Y and Zr/Y from bed 4 may be related to placering or survival of heavy minerals containing Ti, Nb, and Zr. Pyribole, opaque oxides, titanite and zircon could be candidates. Heavy mineral enrichment in beds 2, 1 relative to clays were probably caused by lowered sedimentation rate with less accumulation of clays or feldspar.

Cr, V, Ni, and Cu

Cr shows correlation to TiO₂ and two samples of the beds 2, 1 have the highest values. Ni, V and Cu concentrations were related to TS values in bed 6 (Fig. 4), and they have peak in this bed. Thus Cr is immobile under variable redox condition relative to V, Ni and Cu in the examined samples. Cr/Zr correlates to variation of Ti/Zr, excluding beds 2, 1 (Fig. 3). In beds 6 and 5, Cr/Zr show relatively less variation than that of Ti/Zr, suggestive existence of heavy minerals such as cromite which may behave similarly to zircon in sedimentary process (Taylor and McLennan, 1985; McLennan et al., 1993).

Weathering condition

To evaluate degrees of weathering, the chemical compositions of sedimentary rocks are plotted as molar proportions within Al₂O₃–(CaO*+Na₂O)–K₂O (A–CN–K) compositional space, where CaO* represents Ca in silicate-bearing minerals only (Nesbitt and Young, 1989; Fedo et al., 1995). The CIA (=Al/(Al+Ca+Na+K) × 100, Nesbitt and Young, 1982) is a useful tool for evaluation of weathering, particularly the conversion of feldspar to secondary clay minerals such as kaolinite and illite (Fig. 5).

On this diagram, mud samples plot in a very small area, showing high CIA values (over 80) and significantly homogeneous composition. Supposition of a trend from source rock to this composition parallel to A–CN join is difficult, for their highly nature of CIA may be related to sorting effect as indicated by Nesbitt et al. (1996).

Data set of the Holocene muds (Asakumi Forma-

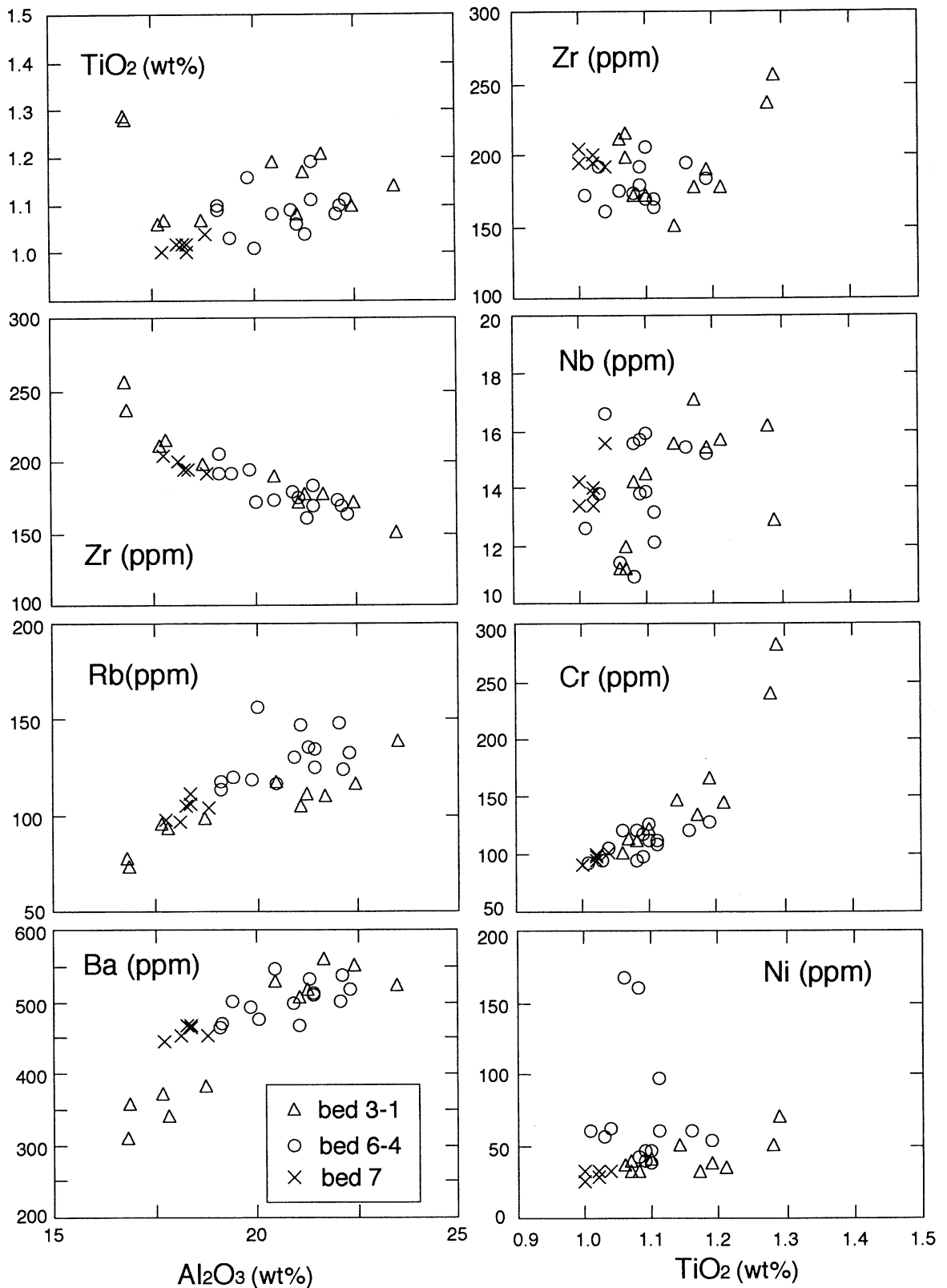


Fig. 4 TiO₂ (wt%), Zr (ppm), Rb (ppm) and Ba (ppm) vs. Al₂O₃ (wt%), and Zr, Nb (ppm), Cr (ppm) and Ni (ppm) vs. TiO₂ for mud samples at the archeological site in Shimane University (SU section), San'in district of Southwest Japan.

tion) from the archeological site along the Asakumi River plots on the line parallel to the A-CN join with CIA ranging from 76 to 85. Samples of the SU section lie on the end of this trend, suggesting they were derived from same source material similar to the Daito granodiorite.

Weak CIA variation in bed 6 correlates with change

in Rb/k ratio. Rb/K fluctuation in bed 6 may be related to Rb enrichment due to adsorption of Rb on clays under marine condition.

Comparison with other Holocene mud composition

Holocene mud composition has been also examined at archeological site along the present Asakumi River

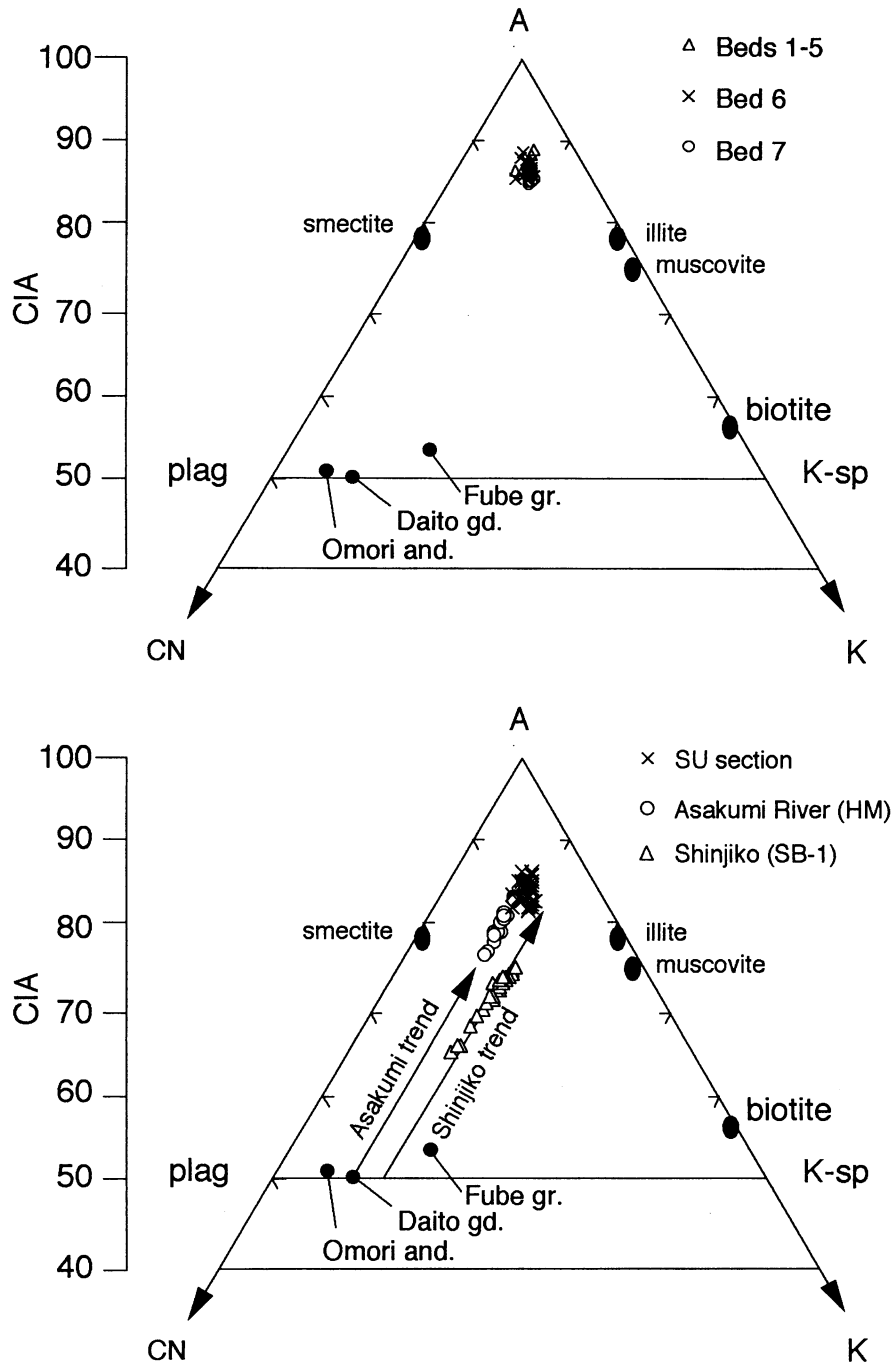


Fig. 5 Al₂O₃–(CaO+Na₂O)–K₂O diagram and CIA (chemical index of alteration) for the muds at the archeological site in Shimane University (SU section), San’in district of Southwest Japan. Compositions of granites (Fube granite), granodiorite (Daito granodiorite) and Omori (Omori andesite) are also given for estimation of source composition. The Omori andesite is intercalated in the Tertiary rocks. Data from Kano et al. (1994).

(HM; Haranomae remain of Tokuoka et al., 1995), and core samples in the Lake Shinji (SB-1 of Tokuoka et al., 1990). Analytical results are shown in Table 2 in average values and STD.

Plots on the A-CN-K diagram show that SB-1 samples lie on different trend from the Asakumi trend (HM samples) with supposed source composition which occurs between the Daito granodiorite and Fube granite (Fig. 4). They are more silicic and have lower CIA (65-75) relative to samples of the HM section and SU section.

To evaluate difference of these Holocene mud composition, elements of the SU and HM samples are normalized by average values of the Holocene of the SB-1 core samples.

The enrichment and depletion for any element x (Ex^*) is given by the following equation:

$$Ex^* = (C_x \text{ sample} / C_{Al} \text{ sample}) / (C_x \text{ standard} / C_{Al} \text{ standard})$$

where: C_x sample is concentration of the element in the sample and C_{Al} sample is the sample Al content. C_x standard and C_{Al} standard are equivalent quantities for average values of the SB-1 samples.

SU and HM samples show similar patterns in this factor (Fig. 6). TiO_2 , Cr, and Ni are enriched relative to SB-1 samples, while most alkali and alkaline earth elements are depleted compared with SB-1 muds, excluding Sr and Ba. Zr is most enriched in HM samples, and Y and Nb are slightly enriched in both SU and HM samples. Depletion in most alkali and alkaline earth elements relative to SB-1 samples show highly weathered nature of mud composition.

TiO_2 , Cr and Ni concentration compared with SB-1 is suggestive of more mafic source for the sediments of the Asakumi fluvial system. Mud of the SB-1 may be related to local granites and granodiorites

which are distributed in the Chugoku mountain regions (Editorial Board of Geological Map of Shimane Prefecture, 1982), while sediments of the Asakumi fluvial system have the provenance composed of Tertiary sediment and volcanic complexes. This may be significant for chemical composition. This implies that reworking of sedimentary rocks may result in relatively higher CIA, and may have an effect of immobile element concentration during sedimentary process. Lower sedimentation rate in the SU section may accentuate this effect and concentrated Al_2O_3 , TiO_2 , Cr and Zr during weathering process. SiO_2 , CaO, Na_2O , K_2O , Sr and Zr enrichment in the HM samples may be due to grain size effect on composition compared with SU samples.

SU muds, however, show similar composition to HM samples, derived from the provenance of the Asakumi River system, while SB-1 of Shinjiko samples may represent more felsic source terrane of the Hii River system.

Acknowledgements

Yoshihiro Sawada of Shimane University kindly provided the XRF facilities. Kazuhiro Ege of Shimane University contributed valuable guidance on the archaeological remains at the SU section. Part of the samples of SU section was prepared for analysis by Seiji Yokoyama of Shimane University.

Part of the investigation was supported by a Grant-in-Aid from the Ministry of Education, Science and Culture of Japan.

References

- Berner, R. A., 1984. Sedimentary pyrite formation: An updated. *Geochim. Cosmochim. Acta*, **48**, 605-615.
 Berner, R. A. and Raiswell, R., 1984. C/S method for

Table 2 Average values of the muds in HM section (Haranomae remain in the Asakumi River) and Holocene muds in the SB-1 section of the Shinji Lake, San'in district of Southwest Japan. Analysis of USGS standard shale SCo-1 (Cody Shale) is also given with preferred values (p.v.) for comparison.

samples	Oxides (wt. %)											Trace elements (ppm)											
	SiO ₂	TiO ₂	Al ₂ O ₃	Fe ₂ O ₃	MnO	MgO	CaO	Na ₂ O	K ₂ O	P ₂ O ₅	Total	V	Cr	Ni	Cu	Zn	Y	Zr	Nb	Rb	Sr	Ba	
Lake Shinji (SB-1)																							
Av. (n=38)	64.65	0.86	19.22	6.65	0.09	2.29	0.73	1.97	2.68	0.12	99.25	125	63	28	15	116	28	155	12	138	114	293	
STD	4.03	0.03	1.33	1.82	0.01	0.47	0.05	0.16	0.18	0.00		14.9	6.9	5.2	2.4	18.7	0.8	26.8	2.3	5.3	1.6	75.9	
Asakumi River																							
Av. (n=28)	72.41	0.98	16.66	5.39	0.05	1.36	0.65	1.09	1.80	0.06	100.46	92	104	40	14	79	27	210	12	76	136	396	
STD	0.721	0.09	1.54	0.33	0.00	0.37	0.18	0.11	0.50	0.03		11.0	1.1	14.3	11.0	22.3	6.6	59.9	0.4	12.0	39.6	37.1	
SCo-1																							
p.v.	64.13	0.64	13.96	5.25	0.05	2.78	2.68	0.92	2.83	0.21	93.45	134	69	28	29	105	27	163	11	114	178	582	
av. (n=6)	65.18	0.62	13.93	5.45	0.05	2.68	2.60	1.41	2.77	0.37	95.08	120	73	29	24	106	21	172	14	124	171	544	
STD	0.32	0.00	0.09	0.02	0.00	0.02	0.01	0.04	0.01	0.01		4.8	2.5	0.6	4.3	1.1	0.5	0.6	0.2	0.2	0.1	7.7	

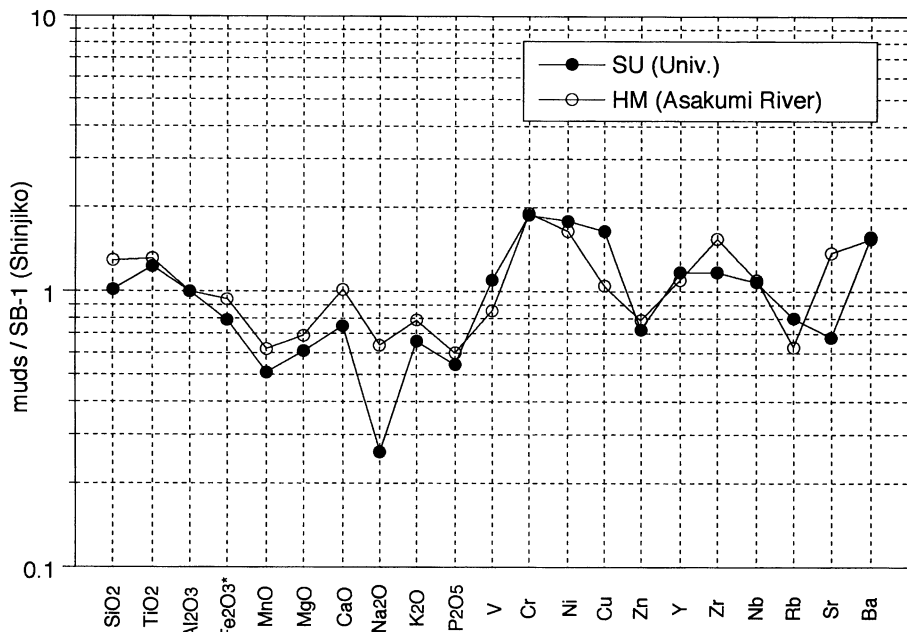


Fig. 6 Average enrichment factor diagram for the Holocene sediments in the SU (Shimane University) and HM (Haranomae remain in the Asakumi River) sections, normalized by Holocene sediments of the SB-1 core samples from the Shinji lagoon, San'in district, SW Japan.

distinguishing freshwater from marine sedimentary rocks. *Geology*, 12, 365-368.

Fedo, C. M., Nesbitt, H. W. and Young, G. N., 1995. Unraveling the effects of potassium metasomatism in sedimentary rocks and paleosols, with implications for paleoweathering conditions and provenance. *Geology*, 23, 921-924.

Editorial Board of Geological Map of Shimane Prefecture, 1982. Geological map of Shimane Prefecture (1:200,000).

Garcia, D., Fonteiller, S. M. and Moutte, J., 1994. Sedimentary fractionations between Al, Ti, and Zr and genesis of strongly peraluminous granites. *Jour. Geol.*, 102, 411-422.

Kano, K., Yamauchi, S., Takayasu, K., Matsuura, H. and Bunno, M., 1994. *Geology of the Matsue district. With geological Sheet Map at 1:50,000*. Geol. Surv. Japan, 126 pp.

McLennan S., Hemming S., MacDaniel D.K. and Hanson G.N. (1993) Geochemical approach to sedimentation, provenance and tectonics. *Geol. Soc. Am. Spec. Paper*, 284, 21-40.

Nakamura, T. and Tokuoka, T., 1997. The Akahoya (K-Ah) tephra discovered from the SB-1 drilling in the lake Shinji and reexamination of the Holocene

paleogeographic changes. *Geol. Rept. Shimane Univ.*, 15, 35-40.

Nesbitt, H. W. and Young, G. M., 1982. Early Proterozoic climates and plate motions inferred from major element chemistry of lutites. *Nature*, 299, 715-717.

Nesbitt, H. W. and Young, G. M., 1989. Formation and diagenesis of weathering profiles. *Jour. Geol.*, 97, 129-147.

Nesbitt, H. W., Young, G. M., McLennan, S. M. and Keays, R. R., 1996. Effects of chemical weathering and sorting on petrogenesis of siliciclastic sediments, with implications for provenance studies. *Jour. Geol.*, 104, 525-542.

Norrish, H. W. and Hutton, J. T., 1969. An accurate X-ray spectrographic method for the analysis of a wide range of geologic samples. *Geochim. Cosmochim. Acta*, 33, 431-453.

Ota, Y. and Yonekura, N., 1987. Quaternary Maps of Japan II Prehistoric Remains and Paleogeography. Japan Association of Quaternary Research (eds.), Tokyo Univ. Press.

Ota, Y., Matsushima, Y. and Moriwaki, H., 1982. Note on the Holocene sea-level study in Japan.— On the basis of “Atlas of Holocene sea-level records in

- Japan”-. *Quat. Res.*, **21**, 133-143.
- Potts, P. J., Tindle, A. G. and Webb, P. C., 1992. *Geochemical reference material compositions*. Whit-tles Publishing, 313 pp.
- Sampei, Y., 1991. CHN-corder. *Earth Sci.*, **45**, 285-289.
- Sampei, Y., Matsumoto, E., Kamei, T. and Tokuoka, T., 1997. Sulfur and organic carbon relationship in sediments from coastal brackish lakes in the Shi-mane peninsula district, southwest Japan. *Geochem. Jour.*, **31**, 245-262.
- Sampei, Y., Matsumoto, E., Tokuoka, T. and Inoue, D., 1996. Organic carbon accumulation rate during the last 8,000 years in lake Nakaumi, Southwest Japan: Coastal lagoon sediments as carbon sink. *Quat. Res.*, **35**, 113-124.
- Suzuki, N., Yamamoto, J., Muranaka, H., Takayasu, K., Yamauchi, S., Onishi, Y., Tokuoka, T., Shi-mada, I., Mitsunashi, T., 1986. Analysis of geologi-cal materials by YANAKO CHN corder (MT 3) I.-determination of sedimentary organic carbon by low temperature combustion method and acid treat-ment-combustion method, and its use on line with Personal Computer. *Geol. Rep. Shimane. Univ.*, **5**, 19-34.
- Taylor, S. R. and McLennan, S. M., 1985. *The Conti-nental Crust: its composition and evolution*. Black-well, Oxford, 312 pp.
- Terashima, S., 1979. The determination of total car-bon, total sulfur, carbonate and non-carbonate in geological materials by infrared absorption spec-trometry. *Bull. Geol. Surv. Japan*, **30**, 609-627.
- Tokuoka, T., Onishi, Y., Nakamura, T. and Takayasu, K., 1995. Paleoenvironment of the Haranomae ar-cheological site and its neighbor, San'in district, Southwest Japan. In *Haranomae Archeological Re-mains*, Board of Education, Shimane Prefectural Of-fice, 181-195.
- Tokuoka, T., Onishi, Y., Takayasu, K. and Mitsunashi, T., 1990. Natural history and environmental changes of Lakes Nakaumi and Shinji. *Mem. Geol. Soc. Ja-pan*, **36**, 15-34.
- Umitsu, M., 1991. Holocene sea-level changes and coastal evolution of Japan. *Quat. Res.*, **30**, 187-196.

(Received : 24 Sep. 1998, Accepted : 30 Sep. 1998)

(要 旨)

石賀裕明・中村唯史・三瓶良和・徳岡隆夫・高安克己, 1998, 地球化学的にみた西南日本山陰地域の海跡湖堆積物に記録された縄文海進の最大海水準上昇, 島根大学地球資源環境学研究报告, 17, 11-20

完新統の縄文海進の地質学的記録の1つが島根大学にて行われた遺跡発掘現場の地層にみられる。この地点は当時の予想される海岸線の最も湾奥の後背湿地に位置する。堆積物の地球化学的特徴から非海成層から海成層への急激な変化が認められ、その基底にはアカホヤ火山灰(約6,300年前)が挟まれる。したがってこの層準は縄文海進の最大海面上昇を示唆する。海成層は1.3 mあり、その上位には非海成層が重なる。この非海成層は下位の地層に比較して Al_2O_3/TiO_2 , SiO_2/Al_2O_3 , Ti/Zr , Nb/Y , および Zr/Y 比などが変化する。このことは弥生時代に始まる平野の開墾による後背地の変化を示唆する。